

Resonant low-energy electron scattering on short-range impurities in graphene

D. M. Basko*

International School of Advanced Studies (SISSA), via Beirut 2-4, 34014 Trieste, Italy

Resonant scattering of electrons with low energies (as compared to the bandwidth) on a single neutral short-range impurity in graphene is analyzed theoretically, taking into account the valley degeneracy. Resonances dramatically increase the scattering cross-section and introduce a strong energy dependence. Analysis of the tight-binding model shows that resonant scattering is typical for generic impurities as long as they are sufficiently strong (the potential is of the order of the electron bandwidth or higher).

I. INTRODUCTION

Electron transport in graphene is a subject of intense study, both theoretical and experimental, since the very discovery of this material in 2004.¹ In general, electron transport is determined by competition of different scattering mechanisms, both inelastic (e. g., electron-phonon) and elastic (static defects). Elastic scattering is dominant for sufficiently low temperatures.

Different kinds of crystal imperfections can be a source of elastic electron scattering in graphene: mesoscopic corrugations of the graphene sheet (ripples)² producing perturbations smooth on the atomic scale, charged impurities producing long-range Coulomb fields, or short-range neutral impurities. While the first two types seem to be more important for the transport in the clean graphene, it is probably the third one that can be controlled. In Refs. 3,4 graphene oxide was chemically reduced to normal graphene; in Ref. 5 hydrogen and hydroxyl groups were deposited on the graphene sheet in a controlled and reversible manner; in all cases resistance changed by several orders of magnitude. Assuming that attaching a chemical group to a carbon atom in graphene changes the hybridization of its electronic orbitals from sp^2 to sp^3 , one can view such group as a neutral short-range impurity.

Short-range impurities in graphene have received a noticeable amount of theoretical attention recently. Refs. 6, 7,8,9 focused on modification of the local electronic properties (such as the local density of states) in the vicinity of a single impurity. The present work is dedicated to the problem of electron scattering on a single short-range impurity whose size R is assumed to be of the order of the interatomic distance a (the C-C bond length), and the electron energy ϵ is assumed to be much smaller than the energy scale set by the potential, v/R (v is the electron velocity at the Dirac point, so that v/R is of the order of the electronic bandwidth). For particles with parabolic spectrum such low-energy scattering is characterized by a single constant of the dimensionality of length (the scattering length), determined from the solution of the Schrödinger equation at zero energy. In graphene, due to the degeneracy of the spectrum at the Dirac point, more than one length is needed to characterize a scatterer.¹⁰

The common intuition is that for a strong enough scatterer the typical value of scattering lengths $l \sim R$, yield-

ing the cross-section $\sigma \sim pl^2 \ll a$ (here $p = |\epsilon|/v$ is the electron momentum counted from the Dirac point). The exception to this is the case of resonant scattering when the potential has a (quasi-)bound state with small energy, then one of the scattering lengths becomes of the order of the size of this state. The main motivation for the present study is that for the Dirac spectrum the exception becomes a rule: a vacancy (which can be viewed as the limit of an infinitely strong scatterer) introduces a bound state exactly in the Dirac point,^{6,7,8} so one of the scattering lengths diverges. It is hard to introduce a real vacancy in graphene, however, if the π -orbital of some carbon atom is very tightly bound, this atom acts effectively as a vacancy for the rest of the π -electrons in the crystal. In particular, impurities introduced electrochemically^{3,4,5} are likely to act as strong scatterers. This expectation is supported by density-functional theory (DFT) calculations for graphene¹¹ (a hypothetical material obtained from graphene by attaching a hydrogen atom to each carbon): the binding energy was obtained to be about 7 eV per hydrogen atom. For such scatterers the scattering length should be large, thus motivating the present study.

The main framework of this study is the general scattering theory¹² modified for the 2D Dirac equation^{13,14,15,16} taking into account the valley degeneracy. In Sec. III we show that for a general short-range scatterer all the information necessary to determine the cross-section up to corrections of the order $(pR)^2$ is encoded in a 4×4 matrix L and a constant r_0 (all having the dimensionality of length). The terms of the order $(pR)^2$ and higher cannot be studied using the Dirac equation, as the Dirac hamiltonian itself is the leading term in the expansion of a microscopic hamiltonian in the parameter pa (and $R \sim a$ is always assumed here). The matrix L (i) can be obtained from the solution of the microscopic Schrödinger equation for electrons in the graphene crystal at zero energy and with an appropriate asymptotics; (ii) is hermitian and invariant with respect to the time reversal, so it depends on 10 real parameters; (iii) its four eigenvalues play the role of the scattering lengths. Divergence of one or several of these eigenvalues signals the existence of a localized solution at zero energy. For the parameter r_0 we have (i) $r_0 \sim R$; (ii) the dependence of the scattering amplitude on r_0 is weak (logarithmic); (iii) the exact value of r_0 cannot be extracted from the

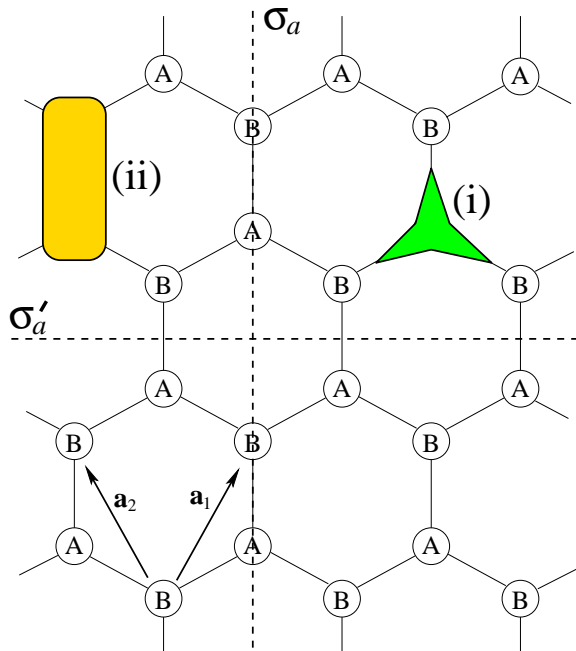


FIG. 1: The honeycomb lattice with two atoms (A and B) per unit cell and the elementary translation vectors \mathbf{a}_1 and \mathbf{a}_2 . The two inequivalent reflection planes σ_a and σ'_a are shown. (i) and (ii) are schematic representations of site-like and bond-like impurities with symmetries C_{3v} and C_{2v} , respectively.

zero-energy solutions only, wave functions at low but finite energies have to be considered in order to determine it.

In Sec. IV we consider two examples of impurities with special symmetries, and see how these symmetries manifest themselves in the scattering (i. e., how they restrict the form of the matrix L). The first example (the site-like impurity) is an impurity localized around one of the carbon atoms and preserving its C_{3v} symmetry (C_{3v} consists of three-fold rotations and reflections in three planes perpendicular to the crystal plane); it is natural to assume that this would be the case for a hydrogen atom bound to a carbon. The second kind (the bond-like impurity) involves two neighboring carbon atoms and the bond between them and has the symmetry C_{2v} . This could be the case for an oxygen atom bound to two carbon atoms. The two kinds of impurities, described above, are schematically shown in Fig. 1. Of course, a generic impurity is not going to have any symmetry at all.

Since graphene crystal is symmetric, impurities of the same kind can occur in different locations and with different orientations with equal probability, if these can be related to each other by a crystal symmetry operation. For example, the site-like impurity, located on an A atom in Fig. 1, can reside on a B atom with the same probability; the bond-like impurity can have one of the three different orientations, rotated by $2\pi/3$ with respect to each other. Although equivalent from the crystal sym-

C_{6v}	E	C_2	$2C_3$	$2C_6$	$\sigma_{a,b,c}$	$\sigma'_{a,b,c}$
A_1	1	1	1	1	1	1
A_2	1	1	1	1	-1	-1
B_2	1	-1	1	-1	1	-1
B_1	1	-1	1	-1	-1	1
E_1	2	-2	-1	1	0	0
E_2	2	2	-1	-1	0	0

TABLE I: Irreducible representations of the group C_{6v} and their characters.

metry point of view, such impurities will have different L matrices. If one is not looking at effects of coherent scattering off several impurities, the cross-section can be averaged over such equally probable impurity configurations. This procedure is described in Sec. V.

In Sec. VI we perform explicit calculations in the tight-binding model for the two kinds of impurities, modeled as a diagonal on-site potential for a site-like impurity, and a combination of a diagonal and an off-diagonal potentials for a bond-like impurity (the same model was adopted in Ref. 8). The scattering lengths are calculated as functions of the impurity strengths, and r_0 is obtained to be $0.5a$. In agreement with the results of Ref. 8, the divergence of the scattering length occurs at infinite impurity strength for a site-like impurity (corresponding to a zero-energy state bound to a vacancy), and at finite values of the diagonal and off-diagonal strengths for a bond-like impurity. The resulting cross-sections as functions of the electron energy for different impurity strengths are shown in Figs. 2,3.

II. FREE ELECTRONS IN GRAPHENE

Graphene unit cell contains two atoms, labelled A and B (Fig. 1). Each of them has one π -orbital, so there are two electronic states for each point of the first Brillouin zone (we disregard the electron spin). The electronic energy ϵ (measured from the Fermi level of the undoped graphene) vanishes at the two Dirac points K, K' with wave vectors $\pm\mathbf{K}$. Thus, there are exactly four electronic states with $\epsilon = 0$. An arbitrary linear combination of them is represented by a 4-component column vector ψ . Being interested in low-energy states, we focus on states in the vicinities of the Dirac points. The wave vectors of these states can be written as $\mathbf{k} = \pm\mathbf{K} + \mathbf{p}$, where $pa \ll 1$ (here $a \approx 1.42 \text{ \AA}$ is the C-C bond length). Equivalently, states near the Dirac points are obtained by including a smooth position dependence $\psi(\mathbf{r})$, $\mathbf{r} \equiv (x, y)$.

The basis in the space of 4×4 hermitian matrices is formed by 16 generators of the $SU(4)$ group. They can be represented as products of two mutually commuting algebras of Pauli matrices $\Sigma_x, \Sigma_y, \Sigma_z$ and $\Lambda_x, \Lambda_y, \Lambda_z$,^{10,17} which fixes their algebraic relations. The convenient way to define these matrices is to specify the irreducible repre-

irrep	A_1	B_1	A_2	B_2	E_1	E_2
valley-diagonal matrices						
matrix	$\mathbb{1}$	Λ_z	Σ_z	$\Lambda_z \Sigma_z$	Σ_x, Σ_y	$-\Lambda_z \Sigma_y, \Lambda_z \Sigma_x$
valley-off-diagonal matrices						
matrix	$\Lambda_x \Sigma_z$	$\Lambda_y \Sigma_z$	Λ_x	Λ_y	$\Lambda_x \Sigma_y, -\Lambda_x \Sigma_x$	$\Lambda_y \Sigma_x, \Lambda_y \Sigma_y$

TABLE II: Classification of 4×4 hermitian matrices by irreducible representations of the C_{6v} group. Matrices joined by braces transform through each other under translations.

resentation of the C_{6v} group, the point group of graphene, according to which they transform. The irreducible representations of C_{6v} are listed in Table I (C_n denotes the rotation by $2\pi/n$, $\sigma_{a,b,c}$ are the three reflections which swap the K and K' points, $\sigma'_{a,b,c}$ are the three reflections which swap A and B atoms, the fixed point of these operations being the center of the hexagon, see Fig. 1), the correspondence between them and the matrices is given in Table II. By definition, the isospin Σ_x, Σ_y are the matrices, diagonal in the K, K' subspace, and transforming according to the E_1 representation of C_{6v} . If one chooses the following arrangement of the wave function components in the column,¹⁰

$$\psi = \begin{bmatrix} \psi_{AK} \\ \psi_{BK} \\ \psi_{BK'} \\ -\psi_{AK'} \end{bmatrix}, \quad (1)$$

then Λ_i are the Pauli matrices acting in the ‘‘external’’ subspace of the 2-blocks (the valley subspace), while Σ_i are the Pauli matrices acting within each 2-block (the AB subspace). We also note that $U_{C_3} = e^{(2\pi i/3)\Sigma_z}$ is the matrix of the C_3 rotation, $U_{C_2} = \Lambda_x \Sigma_z$ – of the C_2 rotation, $U_{\sigma'_a} = \Lambda_z \Sigma_x$ – of the σ'_a reflection, $U_{\sigma_a} = \Lambda_y \Sigma_y$ – of the σ_a reflection. The two elementary translations by the vectors $\mathbf{a}_1, \mathbf{a}_2$ act on the wave function as $t_{\mathbf{a}_{1,2}} : \psi(\mathbf{r}) \mapsto e^{\mp(2\pi i/3)\Lambda_z} \psi(\mathbf{r} - \mathbf{a}_{1,2})$. The time reversal operation is defined as $\psi \mapsto U_t \psi^*$, where the unitary time reversal matrix $U_t = \Sigma_y \Lambda_y$ in the representation (1). The

unit 4×4 matrix is denoted by $\mathbb{1}$, and sometimes Σ_0 or Λ_0 to make the formulas compact.

Taking the leading-order term in the expansion of the band hamiltonian in the powers $pa \ll 1$, we describe the electrons by the Dirac hamiltonian

$$H_0 = -iv\mathbf{\Sigma} \cdot \nabla, \quad (2)$$

where $\mathbf{\Sigma} = (\Sigma_x, \Sigma_y)$ is a two-dimensional vector, and $v \approx 10^8$ cm/s is the electron velocity. The eigenstates of the Dirac hamiltonian with a definite value of momentum are plane waves:

$$\psi_{\mathbf{p}s\kappa}^{(0)}(\mathbf{r}) = e^{i\mathbf{p}\mathbf{r}} \psi_{\varphi_{\mathbf{p}s\kappa}}^{(0)}, \quad (3a)$$

$$\psi_{\varphi_{\mathbf{p}s\kappa}}^{(0)} = \frac{1}{\sqrt{2}} \begin{bmatrix} s e^{-i\varphi/2} \\ e^{i\varphi/2} \end{bmatrix} \otimes \phi_\kappa = W_\varphi^\dagger \frac{1}{2} \begin{bmatrix} 1+s \\ 1-s \end{bmatrix} \otimes \phi_\kappa, \quad (3b)$$

with the energy $\epsilon_{\mathbf{p}s\kappa} = svp$. The index $s = \pm 1$ distinguishes between the conduction and the valence band. The index $\kappa = K, K'$ labels the valleys, and the 2-columns ϕ_κ represent a basis in the degenerate valley subspace: $\Lambda_z \phi_K = \phi_K$, $\Lambda_z \phi_{K'} = -\phi_{K'}$, while the structure in the AB subspace is shown explicitly. The unitary matrices $W_{\varphi_{\mathbf{p}}} = e^{i\Sigma_y \pi/4} e^{i\Sigma_z \varphi_{\mathbf{p}}/2}$, where $\varphi_{\mathbf{p}} = \arctan(p_y/p_x)$ is the polar angle of the vector \mathbf{p} , diagonalize the Dirac hamiltonian in the momentum representation: $v\mathbf{p} \cdot \mathbf{\Sigma} = W_{\varphi_{\mathbf{p}}}^\dagger v p \Sigma_z W_{\varphi_{\mathbf{p}}}$.

Besides plane waves, we will need the wave functions of states with a definite half-integer value of the ‘‘total angular momentum’’ $j_z = -i(\partial/\partial\varphi) + (1/2)\Sigma_z$ which also commutes with the Dirac hamiltonian (2):

$$\psi_{p j_z s \kappa}^{(0)}(\mathbf{r}) = \frac{1}{\sqrt{2}} \begin{bmatrix} s J_{j_z - 1/2}(pr) e^{i(j_z - 1/2)(\varphi + \pi/2)} \\ J_{j_z + 1/2}(pr) e^{i(j_z + 1/2)(\varphi + \pi/2)} \end{bmatrix} \otimes \phi_\kappa, \quad (4)$$

where J_m are Bessel functions of the first kind. If one relaxes the condition of regularity of the wave function at $\mathbf{r} = 0$, the Bessel functions of the first kind J_m can be replaced by the Bessel functions of the second kind Y_m , or Hankel functions $H_m^{(1,2)} = J_m \pm iY_m$.

III. RESONANT SCATTERING ON A SHORT-RANGE POTENTIAL

A. General definitions

Here we use the standard expansion in partial waves¹² modified for the Dirac equation analogously to Refs. 13,14, 15,16. For a potential $V(\mathbf{r})$ that falls off rapidly at distances $r \gtrsim R$, the electron motion at distances $r \gg R$ can be considered free. The general scattering solution corresponding to the energy $\epsilon = svp$ can be written as

$$\begin{aligned} \psi_{\mathbf{p}s\kappa}(\mathbf{r}) &= \sum_{m=-\infty}^{\infty} \frac{e^{-i(m+1/2)\varphi_{\mathbf{p}}}}{\sqrt{2}} \begin{bmatrix} s J_m(pr) e^{im(\varphi + \pi/2)} \\ J_{m+1}(pr) e^{i(m+1)(\varphi + \pi/2)} \end{bmatrix} \otimes \phi_\kappa + \\ &+ \sum_{m=-\infty}^{\infty} \frac{1}{\sqrt{2}} \begin{bmatrix} s H_m^{(1)}(pr) e^{im(\varphi + \pi/2)} \\ H_{m+1}^{(1)}(pr) e^{i(m+1)(\varphi + \pi/2)} \end{bmatrix} \otimes \frac{1}{2} \mathcal{F}_{m+1/2}^s(\mathbf{p}) \phi_\kappa. \end{aligned} \quad (5)$$

The first sum represents just the incident plane wave (3b). The second sum in Eq. (5) with an arbitrary 2×2 matrix $\mathcal{F}_{m+1/2}^s(\mathbf{p})$, acting in the Λ -subspace, represents the outgoing scattered wave (the factor $1/2$ in front of \mathcal{F} is introduced for convenience).¹⁹ From the asymptotic behaviour of $H_m^{(1)}(pr)$ at $pr \gg |m^2 - 1/4|$ for integer m ,

$$H_m^{(1)}(pr) \underset{pr \rightarrow \infty}{\sim} \sqrt{\frac{2/\pi}{pr}} e^{ipr - im\pi/2 - i\pi/4}, \quad (6)$$

we deduce the asymptotic behavior of the wave function and determine the scattering amplitude $f_s(\varphi, \varphi_{\mathbf{p}}; p)$, the differential cross-section $d\sigma_{s\kappa\kappa'}(\varphi, \varphi'; p)$ for an incident particle with momentum $\mathbf{p} = (p \cos \varphi', p \sin \varphi')$ in the valley κ' to be scattered into the valley κ in the direction $\mathbf{n} = (\cos \varphi, \sin \varphi)$, and the scattering matrix $\mathcal{S}_s(\varphi, \varphi'; p)$:

$$\psi_{\mathbf{p}s\kappa}(\mathbf{r}) \underset{r \rightarrow \infty}{\sim} e^{i\mathbf{p}\mathbf{r}} \psi_{\varphi_{\mathbf{p}s\kappa}}^{(0)} + \frac{e^{ipr + i\pi/4}}{\sqrt{r}} f_s(\varphi_{\mathbf{r}}, \varphi_{\mathbf{p}}; p) \psi_{\varphi_{\mathbf{r}s\kappa}}^{(0)}, \quad (7a)$$

$$f_s(\varphi, \varphi'; p) = \frac{\mathcal{F}^s(\varphi, \varphi'; p)}{i\sqrt{2\pi p}}, \quad (7b)$$

$$\frac{d\sigma_{s\kappa\kappa'}(\varphi, \varphi'; p)}{d\varphi} = |\phi_{\kappa}^\dagger f_s(\varphi, \varphi'; p) \phi_{\kappa'}|^2, \quad (7c)$$

$$\psi_{\mathbf{p}s\kappa}(\mathbf{r}) \underset{r \rightarrow \infty}{\sim} \frac{e^{-ipr + i\pi/4}}{\sqrt{2\pi pr}} 2\pi\delta(\varphi_{\mathbf{r}} - \varphi_{\mathbf{p}} - \pi) \psi_{\varphi_{\mathbf{p}s\kappa}}^{(0)} + \frac{e^{ipr - i\pi/4}}{\sqrt{2\pi pr}} \mathcal{S}_s(\varphi_{\mathbf{r}}, \varphi_{\mathbf{p}}; p) \psi_{\varphi_{\mathbf{r}s\kappa}}^{(0)}, \quad (7d)$$

$$\mathcal{S}_s(\varphi, \varphi'; p) = \mathbb{1}_{2 \times 2} 2\pi\delta(\varphi - \varphi') + \mathcal{F}^s(\varphi, \varphi'; p), \quad (7e)$$

$$\mathcal{F}^s(\varphi, \varphi_{\mathbf{p}}; p) \equiv \sum_{m=-\infty}^{\infty} \mathcal{F}_{m+1/2}^s(\mathbf{p}) e^{i(m+1/2)\varphi}. \quad (7f)$$

Note that $\psi_{\varphi+2\pi, s\kappa}^{(0)} = -\psi_{\varphi s\kappa}^{(0)}$; the above definitions imply $0 \leq \varphi_{\mathbf{r}} - \varphi_{\mathbf{p}} < 2\pi$. For $-2\pi \leq \varphi_{\mathbf{r}} - \varphi_{\mathbf{p}} < 0$ we have to set $\mathcal{S}_s(\varphi, \varphi'; p) = -\mathcal{S}_s(\varphi + 2\pi, \varphi'; p)$. The scattering matrix satisfies the unitarity and reciprocity conditions. The latter assumes the symmetry of the scattering potential with respect to the time reversal:

$$\int_0^{2\pi} \frac{d\varphi}{2\pi} \mathcal{S}_s^\dagger(\varphi, \varphi_1; p) \mathcal{S}_s(\varphi, \varphi_2; p) = \mathbb{1}_{2 \times 2} 2\pi\delta(\varphi_1 - \varphi_2), \quad (8a)$$

$$\mathcal{S}_s(\varphi, \varphi'; p) = \Lambda_y \mathcal{S}_s^T(\varphi' + \pi, \varphi + \pi; p) \Lambda_y, \quad (8b)$$

where \mathcal{S}^T denotes the transpose of the matrix \mathcal{S} . The scattering amplitude can be related to the T -matrix $T(\mathbf{p}, \mathbf{p}'; \epsilon)$ on the mass shell, $|\mathbf{p}| = |\mathbf{p}'| = |\epsilon|/v$. Starting from the exact expression for the scattered wave function,

$$\psi_{\mathbf{p}s\kappa}(\mathbf{r}) = e^{i\mathbf{p}\mathbf{r}} \psi_{\varphi_{\mathbf{p}s\kappa}}^{(0)} + \int \frac{d^2\mathbf{p}'}{(2\pi)^2} e^{i\mathbf{p}'\mathbf{r}} G(\mathbf{p}', svp) T(\mathbf{p}', \mathbf{p}; svp) \psi_{\varphi_{\mathbf{p}s\kappa}}^{(0)}, \quad G(\mathbf{p}, \epsilon) \equiv \frac{\epsilon \mathbb{1} + v\mathbf{p} \cdot \boldsymbol{\Sigma}}{\epsilon^2 - (vp - i0^+)^2}, \quad (9)$$

and taking its $pr \gg 1$ asymptotics, we arrive at [$\mathbf{n} = (\cos \varphi, \sin \varphi)$ and $\mathbf{n}' = (\cos \varphi', \sin \varphi')$ are unit vectors]:

$$W_\varphi T(p\mathbf{n}, p\mathbf{n}'; svp) W_{\varphi'}^\dagger = \frac{iv}{p} \frac{\mathbb{1} + s\Sigma_z}{2} \otimes s\mathcal{F}^s(\varphi, \varphi'; p). \quad (10)$$

B. Scattering lengths

At $r \sim R$ the potential mixes different terms in Eq. (5). The asymptotic behaviour of the Bessel and Hankel functions at $pr \ll \sqrt{|m| + 1}$ for integer m is given by

$$J_m(pr) = \frac{(\text{sign } m)^m}{|m|!} \left(\frac{pr}{2}\right)^{|m|}, \quad (11a)$$

$$H_{m \neq 0}^{(1)}(pr) = \frac{(\text{sign } m)^m |m|!}{i\pi |m|} \left(\frac{2}{pr}\right)^{|m|}, \quad (11b)$$

$$H_0^{(1)}(pr) = 1 + \frac{2i}{\pi} \left(\ln \frac{pr}{2} + \gamma\right), \quad (11c)$$

where $\gamma = 0.5772\dots$ is the Euler-Mascheroni constant. At this stage we make an assumption that all terms constituting the scattered wave in Eq. (5) should be of the same order at $r \sim R$, provided that *their coupling is allowed by the symmetry of the scattering potential*. Depending on the symmetry of the scattering potential, we have to consider two cases. (i) The potential is isotropic and Σ_z -conserving: $V(\mathbf{r}) = V(r)$, $\Sigma_z V(\mathbf{r}) \Sigma_z = V(\mathbf{r})$ (this case was analyzed in Refs. 13,14,15). Then $j_z = -i(\partial/\partial\varphi) + (1/2)\Sigma_z$ is conserved, so the terms in Eq. (5) with different values of m are decoupled (each term with a given m corresponds to $j_z = m + 1/2$). Matching the terms gives $\mathcal{F}_{j_z} \sim (pR)^{2|j_z|}$. (ii) The potential $V(\mathbf{r})$ is generic, so it mixes all states with different values of j_z . Matching the terms gives $\mathcal{F}_{j_z} \sim (pR)^{|j_z|+1/2}$. Thus, $\mathcal{F}_{\pm 1/2}$ are the most important terms in both cases; moreover, as typically $R \sim a$, considering the terms with $|j_z| > 1/2$ would require going beyond the Dirac hamiltonian, since the Dirac hamiltonian itself is the leading term in the expansion in pa .

At $r \ll 1/p$ we can neglect the energy in the Dirac equation, which becomes

$$[-iv\boldsymbol{\Sigma} \cdot \nabla + V(\mathbf{r})]\psi(\mathbf{r}) = 0. \quad (12)$$

At $r \gg R$ this equation admits solutions of the form

$$r^m e^{im\varphi} \begin{bmatrix} 1 \\ 0 \end{bmatrix} \otimes \phi_\kappa, \quad r^{-m} e^{im\varphi} \begin{bmatrix} 0 \\ 1 \end{bmatrix} \otimes \phi_\kappa, \quad (13)$$

which determine the asymptotics of different angular harmonics of the *four* linearly independent zero-energy solutions. Since non-zero angular harmonics of the incident wave in Eq. (5) vanish at $p \rightarrow 0$, we are interested in the solutions of Eq. (12) whose asymptotics can be written as

$$\psi_{01v}(\mathbf{r}) \underset{r \rightarrow \infty}{\sim} \begin{bmatrix} 1 \\ 0 \end{bmatrix} \otimes \phi_\kappa + \frac{e^{i\varphi}}{ir} \begin{bmatrix} 0 \\ 1 \end{bmatrix} \otimes L_{11}\phi_\kappa + \frac{e^{-i\varphi}}{ir} \begin{bmatrix} 1 \\ 0 \end{bmatrix} \otimes L_{21}\phi_\kappa + \sum_{m>1} O\left(\frac{e^{\pm im\varphi}}{r^m}\right), \quad (14a)$$

$$\psi_{02v}(\mathbf{r}) \underset{r \rightarrow \infty}{\sim} \begin{bmatrix} 0 \\ 1 \end{bmatrix} \otimes \phi_\kappa + \frac{e^{i\varphi}}{ir} \begin{bmatrix} 0 \\ 1 \end{bmatrix} \otimes L_{12}\phi_\kappa + \frac{e^{-i\varphi}}{ir} \begin{bmatrix} 1 \\ 0 \end{bmatrix} \otimes L_{22}\phi_\kappa + \sum_{m>1} O\left(\frac{e^{\pm im\varphi}}{r^m}\right), \quad (14b)$$

where each L_{ij} is a 2×2 matrix in the valley subspace, which has to be determined from the solution of the Schrödinger equation at short distances (the factor $1/i$ is introduced for convenience). Let us associate the indices $i, j = 1, 2$ of the 2×2 matrices L_{ij} with the matrix structure in the Σ -subspace, thus combining the four 2×2 matrices L_{ij} into a single 4×4 matrix L . Then the asymptotic behavior of any solution of Eq. (12) at $r \rightarrow \infty$ can be written as:

$$\psi(\mathbf{r}) = \psi^{(0)} + \frac{1}{ir} (\mathbf{n} \cdot \boldsymbol{\Sigma}) L \psi^{(0)} + \sum_{m>1} O\left(\frac{e^{\pm im\varphi}}{r^m}\right), \quad (15)$$

where $\psi^{(0)}$ is an arbitrary 4-column. This equation could also be viewed as the boundary condition on the angular harmonics of the scattering solution (5) at $r \rightarrow 0$; being formed at short distances $r \sim R$, this boundary condition should not depend on ϵ for $|\epsilon| \ll v/R$. However, due to the logarithmic divergence of Hankel function $H_0^{(1)}(pr)$, matching of wave functions should be performed at some $r = r_0 \sim R$. Note that in contrast to the two-dimensional Schrödinger equation, the value of the constant r_0 cannot be determined from the zero-energy solution since the logarithmic function is not a solution of the Dirac equation at zero energy.

Comparing expressions (14) to the scattering solution (5) and using asymptotic expressions (11), we obtain the general possible form of $\mathcal{F}_{\pm 1/2}^s(\mathbf{p})$:

$$\frac{i}{\pi p} \mathcal{F}_{+1/2}^s(\mathbf{p}) = sL_{11} \left[e^{-i\varphi_{\mathbf{p}}/2} + \frac{1}{2} H_0^{(1)}(pr_0) \mathcal{F}_{+1/2}^s(\mathbf{p}) \right] + L_{12} \left[e^{i\varphi_{\mathbf{p}}/2} + \frac{1}{2} H_0^{(1)}(pr_0) \mathcal{F}_{-1/2}^s(\mathbf{p}) \right], \quad (16a)$$

$$\frac{i}{\pi p} \mathcal{F}_{-1/2}^s(\mathbf{p}) = L_{21} \left[e^{-i\varphi_{\mathbf{p}}/2} + \frac{1}{2} H_0^{(1)}(pr_0) \mathcal{F}_{+1/2}^s(\mathbf{p}) \right] + sL_{22} \left[e^{i\varphi_{\mathbf{p}}/2} + \frac{1}{2} H_0^{(1)}(pr_0) \mathcal{F}_{-1/2}^s(\mathbf{p}) \right]. \quad (16b)$$

Solving these equations and comparing the result to Eq. (10), we obtain the general low-energy T -matrix:²⁰

$$T(\epsilon) = \left[\mathbb{1} + \frac{\epsilon}{v} \left(\ln \frac{2v}{r_0|\epsilon|} - \gamma + \frac{i\pi}{2} \right) L \right]^{-1} 2\pi v L, \quad (17)$$

which determines the differential cross-section:

$$\frac{d\sigma_{s\kappa\kappa'}(\varphi, \varphi'; p)}{d\varphi} = \frac{p}{2\pi v^2} \left| (\psi_{\varphi s\kappa}^{(0)})^\dagger T(sv p) \psi_{\varphi' s\kappa'}^{(0)} \right|^2. \quad (18)$$

The matrix L satisfies (i) $L = L^\dagger$ to ensure the unitarity of the scattering matrix (8a), and (ii) $L = U_t L^T U_t^\dagger$ as a consequence of the reciprocity condition (8b). Thus, it has four orthogonal eigenvectors ψ_i : $L\psi_i = l_i\psi_i$, $i = 1, \dots, 4$, and the four eigenvalues l_i play the role of the scattering lengths. The angular dependence of $d\sigma_{s\kappa\kappa'}(\varphi, \varphi'; p)/d\varphi$ is given by the sum of an isotropic term and terms $\propto e^{\pm i\varphi}$, $e^{\pm i\varphi'}$, and $e^{\pm i\varphi \pm i\varphi'}$ (with all four combinations of the signs). The total out-scattering cross-section (i. e., integrated over φ and summed over v) takes the simple form:

$$\sigma_{s\kappa'}^{\text{out}}(\varphi'; p) = \sum_{i=1}^4 \frac{2\pi^2 p |\psi_i^\dagger \psi_{\varphi' s\kappa'}^{(0)}|^2}{[l_i^{-1} - sp \ln(e^\gamma p r_0/2)]^2 + (\pi p/2)^2}. \quad (19)$$

Typically, one assumes that for a strong potential all scattering lengths $l_i \sim R$. However, an explicit calculation for a point defect in the tight-binding model, performed in Sec. VI, shows that one of the lengths l_i (let it be l_1 for definiteness) can become arbitrarily large. The case $l_1 \rightarrow \infty$ corresponds to the existence of a localized solution $\psi(\mathbf{r}) \sim (\mathbf{n} \cdot \boldsymbol{\Sigma})\psi_1/r$ at zero energy.^{6,7,8} In this case the cross-section diverges at $p \rightarrow 0$. Such divergence has been obtained in Ref. 16 for a particular case of a circular void with zigzag edges. Note that even in the case of resonant scattering the scaling $\mathcal{F}_{j_z} \sim (pR)^{|j_z|} \mathcal{F}_{\pm 1/2}$ holds: indeed, at $l_1 \rightarrow \infty$ the coefficients at the $1/r^m$ terms in the wave function of the localized state should scale as R^m , as there is no other length scale in the problem.

IV. IMPURITIES WITH SPECIAL SYMMETRIES

Let us consider two particular kinds of impurities, shown in Fig. 1.

(i) A site-like impurity with the symmetry C_{3v} whose fixed point is located on one of the atoms (let us assume it to be an A atom). Thus, the matrix L should be invariant under the reflection σ_a and the rotation $C'_3 = C_3 t_{\mathbf{a}_1}$ (we remind that the rotation C_3 is around the center of the hexagon). The conditions $L = U_{\sigma_a}^\dagger L U_{\sigma_a}$, $L = U_{C'_3}^\dagger L U_{C'_3}$ together with the time-reversal symmetry restrict the matrix L to

$$L = L_{A_1} \mathbb{1} + L_{B_2} \Lambda_z \Sigma_z + \tilde{L}_E (\Lambda_x \Sigma_x - \Lambda_y \Sigma_y). \quad (20)$$

The eigenvalues and eigenvectors of this family of matrices

are

$$l_{1,2} = L_{A_1} + L_{B_2} \pm 2\tilde{L}_E, \quad l_{3,4} = L_{A_1} - L_{B_2} \quad (21a)$$

$$\psi_{1,2} = \frac{1}{\sqrt{2}} \begin{bmatrix} 1 \\ 0 \\ 0 \\ \pm 1 \end{bmatrix}, \quad \psi_{3,4} = \frac{1}{\sqrt{2}} \begin{bmatrix} 0 \\ 1 \\ \pm 1 \\ 0 \end{bmatrix}. \quad (21b)$$

The T -matrix has the same transformation properties as the matrix L , so it can be written in the same form (20) with the substitution $L \rightarrow T$. Then, according to Eq. (18) the differential intravalley and intervalley cross-sections can be written as

$$\frac{d\sigma_{KK}}{d\varphi} = \frac{p}{2\pi v^2} \left| T_{A_1} \cos \frac{\varphi - \varphi'}{2} + iT_{B_2} \sin \frac{\varphi - \varphi'}{2} \right|^2, \quad (22a)$$

$$\frac{d\sigma_{K'K}}{d\varphi} = \frac{p}{2\pi v^2} |\tilde{T}_E|^2. \quad (22b)$$

(ii) A bond-like impurity with the symmetry C_{2v} whose fixed point is located at the center of a bond (let us assume it to be a bond connecting the two atoms within the same unit cell). Then, the matrix L should be invariant under the reflection σ'_a and the rotation $C'_2 = C_2 t_{\mathbf{a}_1} t_{\mathbf{a}_2}$, which fixes

$$L = L_{A_1} \mathbb{1} + L_{E_2} \Lambda_z \Sigma_x + \tilde{L}_{A_1} \Lambda_x \Sigma_z + \tilde{L}_{E_2} \Lambda_y \Sigma_y, \quad (23a)$$

$$l_{1,2} = (L_{A_1} + \tilde{L}_{E_2}) \pm (L_{E_2} + \tilde{L}_{A_1}), \quad (23b)$$

$$l_{3,4} = (L_{A_1} - \tilde{L}_{E_2}) \pm (L_{E_2} - \tilde{L}_{A_1}), \quad (23c)$$

$$\psi_{1,2} = \frac{1}{2} \begin{bmatrix} \pm 1 \\ 1 \\ 1 \\ \mp 1 \end{bmatrix}, \quad \psi_{3,4} = \frac{1}{2} \begin{bmatrix} 1 \\ \pm 1 \\ \mp 1 \\ 1 \end{bmatrix}. \quad (23d)$$

The differential intravalley and intervalley cross-sections are

$$\frac{d\sigma_{KK}}{d\varphi} = \frac{p}{2\pi v^2} \left| T_{A_1} \cos \frac{\varphi - \varphi'}{2} + sT_{E_2} \cos \frac{\varphi + \varphi'}{2} \right|^2, \quad (24a)$$

$$\frac{d\sigma_{K'K}}{d\varphi} = \frac{p}{2\pi v^2} \left| \tilde{T}_{A_1} \sin \frac{\varphi - \varphi'}{2} + s\tilde{T}_{E_2} \sin \frac{\varphi + \varphi'}{2} \right|^2. \quad (24b)$$

If the location of the impurity is different from what we have assumed, its L matrix can be obtained by applying the corresponding symmetry operation. For example, in case (i) the matrix for an impurity located on a B atom is obtained by a C_2 rotation: $L \rightarrow \Lambda_x \Sigma_z L \Lambda_x \Sigma_z$. Obviously, these two locations can occur with equal probability, so one could average over them. This procedure is described in the next section.

V. AVERAGING OVER THE IMPURITIES

As discussed in the end of the preceding section, the presence of defects characterized by a certain T -matrix $T(\mathbf{p}, \mathbf{p}', \epsilon)$ implies the presence of the same (on average) number of defects of the same type, placed in different locations with different orientations, and thus having different T -matrices, but equivalent with respect to the symmetry of the crystal. If one studies effects which do not involve coherent scattering on several impurities, it is sufficient to average any observable $\mathcal{O}[T(\mathbf{p}, \mathbf{p}', \epsilon)]$, calculated for a single impurity, according to

$$\begin{aligned} \bar{\mathcal{O}} = & \frac{1}{3|C_{6v}|} \sum_{R \in C_{6v}} \left(\mathcal{O} \left[U_R T(R\mathbf{p}, R\mathbf{p}', \epsilon) U_R^\dagger \right] + \right. \\ & + \mathcal{O} \left[U_{t_{a_1}} U_R T(R\mathbf{p}, R\mathbf{p}', \epsilon) U_R^\dagger U_{t_{a_1}}^\dagger \right] + \\ & \left. + \mathcal{O} \left[U_{t_{a_1}}^\dagger U_R T(R\mathbf{p}, R\mathbf{p}', \epsilon) U_R^\dagger U_{t_{a_1}} \right] \right). \end{aligned} \quad (25)$$

Here $|C_{6v}| = 12$ is the number of elements in the C_{6v} group, R are the operations from the group, and U_R are their 4×4 matrices in the ψ -representation. The averaging is performed also over the elementary translations with the matrices $U_{t_{a_1}} = e^{-(2\pi i/3)\Lambda_z}$ and $U_{t_{a_2}} = U_{t_{a_1}}^\dagger$. It is convenient to consider the group C_{6v}'' – the direct product of the point group C_{6v} and the 3-cyclic group represented by the matrices $\mathbb{1}, e^{\pm(2\pi i/3)\Lambda_z}$. Then Eq. (25) describes simply the average over the group C_{6v}'' .

Let us apply this procedure to the differential cross-section. We write the averaged Eq. (18) as

$$\frac{\overline{d\sigma}}{d\varphi} = \frac{p}{2\pi v^2} \sum_{R \in C_{6v}''} \frac{\text{Tr} \{ U_R^\dagger (\psi' \psi'^\dagger) U_R T^\dagger U_R^\dagger (\psi \psi^\dagger) U_R T \}}{|C_{6v}''|}, \quad (26)$$

$$\begin{aligned} \frac{\overline{d\sigma_{s\kappa\kappa'}(\varphi, \varphi'; p)}}{d\varphi} = & \frac{p}{32\pi v^2} \left[\text{Tr} \{ \Lambda_0 T^\dagger(svp) \Lambda_0 T(svp) \} + \frac{1}{2} \cos(\varphi - \varphi') \sum_{j=x,y} \text{Tr} \{ \Lambda_0 \Sigma_j T^\dagger(svp) \Lambda_0 \Sigma_j T(svp) \} \right] + \\ & + (2\delta_{\kappa\kappa'} - 1) [\Lambda_0 \rightarrow \Lambda_z]. \end{aligned} \quad (30)$$

(here we denoted the 4×4 unit matrix $\mathbb{1}$ by Λ_0).

To conclude this section, we note that the averaging procedure described above is equivalent to averaging the cross-section $d\sigma(\varphi, \varphi')/d\varphi$ over $(\varphi + \varphi')/2$ keeping $\varphi - \varphi'$ fixed (due to the symmetry of the crystal with respect to C_3 rotations), and subsequent averaging over the sign of $\varphi - \varphi'$ (due to the symmetry with respect to reflections).

where we abbreviated $\psi = \psi_{\varphi s\kappa}^{(0)}$, $\psi' = \psi_{\varphi' s\kappa'}^{(0)}$, and $T = T(svp)$. Thus, equivalently, we can calculate the average $(\psi' \psi'^\dagger) \otimes (\psi \psi^\dagger)$. In the matrices $\psi \psi^\dagger$ and $\psi' \psi'^\dagger$ we separate the components corresponding to different irreducible representations of C_{6v} :

$$\begin{aligned} \psi \psi^\dagger = & \frac{1}{4} \sum_{i,j=0,x,y,z} (\psi^\dagger \Lambda_i \Sigma_j \psi) \Lambda_i \Sigma_j = \\ = & \frac{1}{4} (\mathbb{1} \pm \Lambda_z) (\mathbb{1} + \mathbf{s}\mathbf{n} \cdot \boldsymbol{\Sigma}), \end{aligned} \quad (27)$$

where the plus (minus) sign should be taken for $\phi_\kappa = \phi_K$ ($\phi_\kappa = \phi_{K'}$), and $\mathbf{n} = (\cos \varphi, \sin \varphi)$. Let us label the matrices $\Lambda_i \Sigma_j$ belonging to an irreducible representation r of the dimensionality d_r as $(\Lambda \Sigma)_\ell^r$, where the index $\ell = 1, \dots, d_r$ labels the matrices within the representation. Then in each representation we can define the $d_r \times d_r$ matrices $(U_R^r)_{\ell\ell'}$ as

$$U_R^\dagger (\Lambda \Sigma)_\ell^r U_R = \sum_{\ell'=1}^{d_r} (U_R^r)_{\ell\ell'} (\Lambda \Sigma)_{\ell'}^r. \quad (28)$$

From the orthogonality relation for the representation matrices¹⁸

$$\frac{1}{|C_{6v}|} \sum_{R \in C_{6v}} (U_R^r)_{\ell_1 \ell_2}^* (U_R^r)_{\ell_3 \ell_4} = \frac{\delta_{rr'}}{d_r} \delta_{\ell_1 \ell_3} \delta_{\ell_2 \ell_4}, \quad (29)$$

we obtain the general expression:

VI. IMPURITIES IN THE TIGHT-BINDING MODEL

A. Green's function

Let us consider the tight-binding model with nearest-neighbor coupling as an exactly solvable example of a microscopic model (i. e., well-defined at short distances). The only parameter of the clean hamiltonian is the nearest-neighbor matrix element which we write as $-2v/(3a)$, thus expressing it in terms of the electron

velocity at the Dirac point. It is convenient to work with a 2-component wave function $\{\Psi_A(\mathbf{r}_n), \Psi_B(\mathbf{r}_n)\}$ (corresponding to the two atoms in the unit cell), where the position of the unit cell $\mathbf{r}_n = n_1 \mathbf{a}_1 + n_2 \mathbf{a}_2$ is labelled by two integers n_1, n_2 . The tight-binding hamiltonian $\mathcal{H}_0(\mathbf{r}_n - \mathbf{r}_{n'})$ is a 2×2 matrix in the sublattice space.

The scattering problem in the tight-binding model with a few-site potential \mathcal{U} is conveniently solved using Lippmann-Schwinger equation (which was used in Refs. 7,8 as well):

$$\Psi = \Psi^{(0)} + \mathcal{G}(\epsilon) \mathcal{U} \Psi, \quad (31)$$

where $\Psi^{(0)}$ is the incident wave, Ψ is the sought wave function, and $\mathcal{G}(\epsilon) = (\epsilon - \mathcal{H}_0)^{-1}$ is the Green's function, explicitly given by

$$\mathcal{G}(\mathbf{r}_n - \mathbf{r}_{n'}, \epsilon) = \int \frac{d^2 \mathbf{k}}{A_{BZ}} \frac{e^{i\mathbf{k}(\mathbf{r}_n - \mathbf{r}_{n'})}}{\epsilon^2 - |t_{\mathbf{k}}|^2} \begin{pmatrix} \epsilon & -t_{\mathbf{k}} \\ -t_{\mathbf{k}}^* & \epsilon \end{pmatrix}, \quad (32)$$

$$t_{\mathbf{k}} = \frac{2v}{3a} (1 + e^{-i\mathbf{k}\mathbf{a}_1} + e^{-i\mathbf{k}\mathbf{a}_2}),$$

$$A_{BZ} \equiv \frac{(2\pi)^2}{A_{uc}} = \frac{(2\pi)^2}{\sqrt{27}a^2/2}.$$

The large-distance behavior of $\mathcal{G}(\mathbf{r}, \epsilon)$ is determined by the singularities of the denominator, i. e., vicinities of the Dirac points $\pm \mathbf{K}$, $\mathbf{k} = \pm \mathbf{K} + \mathbf{p}$, where we can approximate

$$1 + e^{-i(\pm \mathbf{K} + \mathbf{p})\mathbf{a}_1} + e^{-i(\pm \mathbf{K} + \mathbf{p})\mathbf{a}_2} \approx \frac{3a}{2} (\mp p_x + ip_y). \quad (33)$$

Focusing at $|\epsilon| \ll v/a$, we obtain for $r \gg a$ (c. c. stands for the complex conjugate):

$$\mathcal{G}_{AA}(\mathbf{r}, \epsilon) = \frac{A_{uc}|\epsilon|}{4iv^2} (e^{i\mathbf{K}\mathbf{r}} + e^{-i\mathbf{K}\mathbf{r}}) sH_0^{(1)}(|\epsilon|r/v), \quad (34a)$$

$$\mathcal{G}_{BA}(\mathbf{r}, \epsilon) = \frac{A_{uc}|\epsilon|}{4iv^2} (e^{i\mathbf{K}\mathbf{r} + i\varphi + i\pi/2} + \text{c. c.}) H_1^{(1)}(|\epsilon|r/v), \quad (34b)$$

$$\mathcal{G}_{BA}(\mathbf{r}, 0) = \frac{A_{uc}}{v} \frac{e^{i\mathbf{K}\mathbf{r} + i\varphi} - e^{-i\mathbf{K}\mathbf{r} - i\varphi}}{2\pi i r}. \quad (34c)$$

We also need the Green's function at coinciding points:

$$\mathcal{G}_{AA}(\mathbf{0}, \epsilon) = -\frac{A_{uc}\epsilon}{\pi v^2} \left(\ln \frac{2v}{|\epsilon|r_0} - \gamma + \frac{i\pi}{2} \right) + O(\epsilon^3), \quad (35a)$$

$$\mathcal{G}_{BA}(\mathbf{0}, \epsilon) = \frac{a}{2v} + O(\epsilon^2). \quad (35b)$$

The value of r_0 in Eq. (35a) is determined by the integration over the whole first Brillouin zone; numerical integration gives $e^\gamma r_0 = a$ within the numerical precision. The leading term in Eq. (35b) can be easily obtained in the coordinate representation using the fact that \mathcal{H}_0^{-1} , just like \mathcal{H}_0 , is invariant under C_3 rotations around each carbon atom.

B. One-site impurity

Let us add the on-site potential U_0 different from zero only on the A atom of the $n_1 = n_2 = 0$ unit cell. The limit $U_0 \rightarrow \infty$ is equivalent to imposing the boundary condition $\Psi_A(\mathbf{0}) = 0$ and thus describes a vacancy.

First of all, we note that the two plane wave states with $\Psi_A(\mathbf{r}_n) = 0$, $\Psi_B(\mathbf{r}_n) = e^{\pm i\mathbf{K}\mathbf{r}_n}$ remain the zero-energy eigenstates of the hamiltonian even in the presence of the potential. In the representation (1) these two states are represented by the 4-columns

$$\begin{bmatrix} 0 \\ 1 \\ 0 \\ 0 \end{bmatrix} = \begin{bmatrix} 0 \\ 1 \end{bmatrix} \otimes \phi_K, \quad \begin{bmatrix} 0 \\ 0 \\ 1 \\ 0 \end{bmatrix} = \begin{bmatrix} 1 \\ 0 \end{bmatrix} \otimes \phi_{K'}.$$

Comparing them to the asymptotic forms (14), we see that $L_{11}\phi_{K'} = L_{21}\phi_{K'} = 0$, $L_{12}\phi_K = L_{22}\phi_K = 0$.

The other two zero-energy solutions correspond to the incident wave on the A -sublattice, $\Psi_A^{(0)}(\mathbf{r}_n) = e^{\pm i\mathbf{K}\mathbf{r}_n}$, $\Psi_B^{(0)}(\mathbf{r}_n) = 0$. In the representation (1) these two states are represented by the 4-columns

$$\begin{bmatrix} 1 \\ 0 \\ 0 \\ 0 \end{bmatrix} = \begin{bmatrix} 1 \\ 0 \end{bmatrix} \otimes \phi_K, \quad \begin{bmatrix} 0 \\ 0 \\ 0 \\ -1 \end{bmatrix} = \begin{bmatrix} 0 \\ -1 \end{bmatrix} \otimes \phi_{K'}.$$

As the potential U_0 is localized on one atom, and $\mathcal{G}(\epsilon = 0)$ is off-diagonal in the sublattices, the Lippmann-Schwinger equation is straightforwardly solved to give the wave function:

$$\Psi_A(\mathbf{r}_n) = e^{\pm i\mathbf{K}\mathbf{r}_n}, \quad \Psi_B(\mathbf{r}_n) = U_0 \mathcal{G}_{BA}(\mathbf{r}_n, \epsilon = 0). \quad (36)$$

Using Eq. (34c), we obtain

$$L = \frac{A_{uc}U_0}{\pi v} \frac{\mathbf{1} + \Lambda_z \Sigma_z + \Lambda_y \Sigma_y - \Lambda_x \Sigma_x}{4}, \quad (37)$$

in agreement with Eq. (20). The eigenvalues of this matrix are easily found to be $l_1 = A_{uc}U_0/(\pi v)$, $l_2 = l_3 = l_4 = 0$. At $U_0 \rightarrow \infty$ the scattering length l_1 diverges. In this case the amplitude of the incident wave can be set to zero, and $\Psi_B(\mathbf{r}_n) \propto \mathcal{G}_{BA}(\mathbf{r}, \epsilon = 0)$ is the wave function of the state, localized on the vacancy.

At $\epsilon \neq 0$ the Lippmann-Schwinger equation is solved self-consistently for $\Psi_A(\mathbf{0})$ to give the wave functions:

$$\Psi_{\mathbf{k}s}(\mathbf{r}_n) = \begin{pmatrix} e^{i\Phi_{\mathbf{k}}/2} \\ -s e^{-i\Phi_{\mathbf{k}}/2} \end{pmatrix} \frac{e^{i\mathbf{k}\mathbf{r}_n}}{\sqrt{2}} + \frac{e^{i\Phi_{\mathbf{k}}/2}/\sqrt{2}}{U_0^{-1} - \mathcal{G}_{AA}(\mathbf{0}, \epsilon)} \begin{pmatrix} \mathcal{G}_{AA}(\mathbf{r}_n, \epsilon) \\ \mathcal{G}_{BA}(\mathbf{r}_n, \epsilon) \end{pmatrix} \quad (38)$$

where $e^{i\Phi_{\mathbf{k}}} = t_{\mathbf{k}}/|t_{\mathbf{k}}|$. This corresponds to the T -matrix

$$T(\epsilon) = \frac{A_{uc}}{U_0^{-1} - \mathcal{G}_{AA}(\mathbf{0}, \epsilon)} \frac{\mathbf{1} + \Lambda_z \Sigma_z + \Lambda_y \Sigma_y - \Lambda_x \Sigma_x}{2}. \quad (39)$$

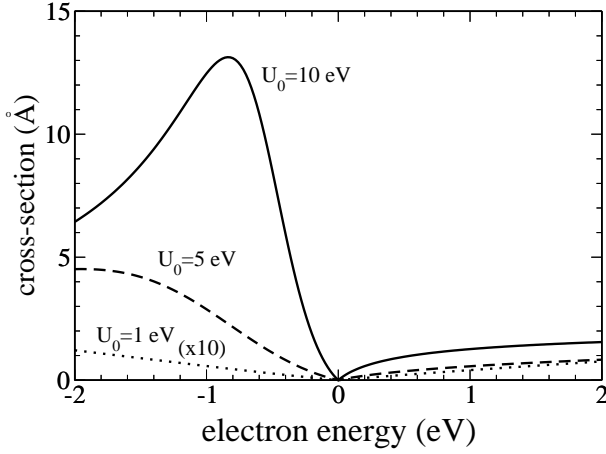


FIG. 2: The out-scattering cross-section (in angstroms) for a one-site impurity of the strength $U_0 = 1, 5, 10$ eV (dotted, dashed, and solid curve, respectively) as a function of the electron energy (in eV), as given by Eq. (40). The curve for $U_0 = 1$ eV is multiplied by a factor of 10. The parameters of the model are $v = 10^8$ cm/s = 6.58 Å, $a = 1.42$ Å.

Using Eq. (35a), we arrive at Eq. (17).

To calculate the average cross-section, we note that in Eq. (30) only the first term survives, so the scattering is isotropic in space and completely mixes the valleys. The total out-scattering cross-section, averaged over the impurity positions, is given by

$$\overline{\sigma^{\text{out}}(\epsilon)} = \frac{\pi^2 v |\epsilon| / 2}{\left(\frac{\pi v^2}{U_0 A_{\text{uc}}} + \epsilon \ln \frac{2v}{e\gamma r_0 |\epsilon|} \right)^2 + \left(\frac{\pi \epsilon}{2} \right)^2}. \quad (40)$$

This cross-section is plotted in Fig. 2 as a function of ϵ for several values of $U_0 = 1, 5, 10$ eV.

C. Two-site impurity

Let us add a potential which mixes the two sites in the $n_1 = n_2 = 0$ unit cell:

$$\mathcal{U} = \begin{pmatrix} U_0 & U_1 \\ U_1 & U_0 \end{pmatrix}. \quad (41)$$

We have chosen U_1 to be real in order to preserve the $A \leftrightarrow B$ symmetry. The self-consistent solution of the Lippmann-Schwinger equation gives

$$\mathcal{U}\Psi(\mathbf{0}) = [\mathcal{U}^{-1} - \mathcal{G}(\mathbf{0}, \epsilon)]^{-1} \Psi^{(0)}(\mathbf{0}) \equiv \mathcal{T}(\epsilon) \Psi^{(0)}(\mathbf{0}). \quad (42)$$

Comparing the resulting wave function with Eq. (15), we obtain

$$L = \frac{A_{\text{uc}}}{2\pi v} \left[\mathcal{T}(0) \frac{\mathbb{1} + \Lambda_z}{2} + \Sigma_y \mathcal{T}(0) \Sigma_y \frac{\mathbb{1} - \Lambda_z}{2} - i\mathcal{T}(0) \Sigma_y \frac{\Lambda_x + i\Lambda_y}{2} + i\Sigma_y \mathcal{T}(0) \frac{\Lambda_x - i\Lambda_y}{2} \right]. \quad (43)$$

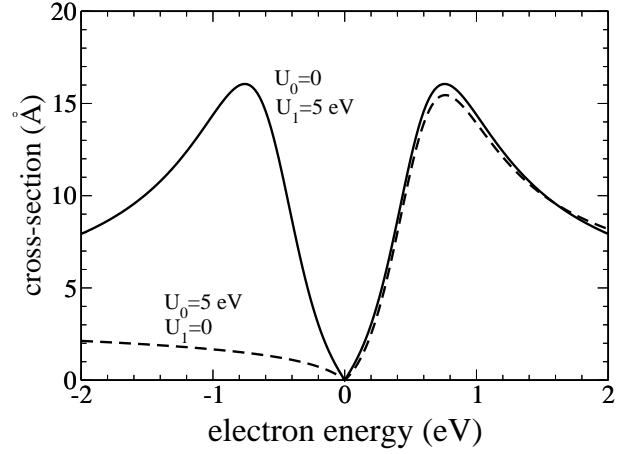


FIG. 3: The out-scattering cross-section (in angstroms) for a two-site impurity with $U_0 = 5$ eV, $U_1 = 0$ (dashed curve), and $U_0 = 0$, $U_1 = 5$ eV (solid curve) as a function of the electron energy (in eV), as obtained from Eq. (45a). The parameters of the model are $v = 10^8$ cm/s = 6.58 Å, $a = 1.42$ Å.

For the potential of the form (41) the scattering lengths are obtained as [the matrix form of L is in agreement with Eq. (23a)]:

$$\begin{aligned} \mathcal{T}(0) &= \frac{(U_0^2 - U_1^2)U_0}{U_0^2 + [U_1 + (a/2v)(U_0^2 - U_1^2)]^2} \mathbb{1} + \\ &+ \frac{(U_0^2 - U_1^2)(U_1 + (a/2v)(U_0^2 - U_1^2))}{U_0^2 - [U_1 + (a/2v)(U_0^2 - U_1^2)]^2} \Sigma_x \equiv \\ &\equiv \mathcal{T}_0 \mathbb{1} + \mathcal{T}_x \Sigma_x, \end{aligned} \quad (44a)$$

$$L = \frac{A_{\text{uc}} \mathcal{T}_0}{2\pi v} (\mathbb{1} + \Lambda_y \Sigma_y) + \frac{A_{\text{uc}} \mathcal{T}_x}{2\pi v} (\Lambda_z \Sigma_x + \Lambda_x \Sigma_z), \quad (44b)$$

$$l_{1,2} = \frac{A_{\text{uc}}}{\pi v} \frac{U_0 \pm U_1}{1 - (a/2v)(U_1 \pm U_0)}, \quad l_{3,4} = 0. \quad (44c)$$

The scattering lengths diverge when $U_1 = 2v/a \pm U_0$, in agreement with the results of Ref. 8.

Calculation of the T -matrix from Eq. (17) and its substitution into Eq. (30) gives the differential intravalley and intervalley cross-section (we set $\varphi' = 0$, as it depends only on $\varphi - \varphi'$):

$$\frac{d\sigma_{\kappa\kappa'}}{d\varphi} = \frac{\pi v |\epsilon|}{8} \left[|t_1|^2 + |t_2|^2 \pm \frac{|t_1 \pm t_2|^2}{2} \cos \varphi \right] \quad (45a)$$

$$t_{1,2}(\epsilon) = \frac{1}{v/l_{1,2} + \epsilon \ln[2v/(e\gamma r_0 |\epsilon|)] + i\pi\epsilon/2}. \quad (45b)$$

In Eq. (45a) the upper and lower sign is taken for the intravalley ($\kappa = \kappa'$) and intervalley ($\kappa \neq \kappa'$) scattering. The total out-scattering cross-section is plotted in Fig. 3 for the two cases of $U_0 = 5$ eV, $U_1 = 0$, and $U_0 = 0$, $U_1 = 5$ eV.

VII. CONCLUSIONS

In this paper we have studied scattering of low-energy electrons on a single neutral short-range impurity in graphene within the framework of the 2D Dirac equation taking into account valley degeneracy. We have shown that for a general short-range scatterer the most important information needed to determine the cross-section is encoded in a 4×4 matrix L , whose eigenvalues are the scattering lengths. Divergence of one or several scattering lengths occurs whenever the impurity has bound electronic states exactly at zero energy, which is accompanied by the singular behavior of the scattering cross-section as a function of the electronic energy. Quasi-bound states manifest themselves as resonances at finite energies, their width determined by the energy itself.

The matrix L can be obtained from the solution of a microscopic model for the impurity in graphene; only the zero-energy states need to be considered for this. As

an example of a microscopic model we take the tight-binding model and calculate the scattering lengths for the diagonal one-site impurity potential and the two-site potential having both diagonal and off-diagonal components. In agreement with the results of Refs. 6,7,8,9 for the impurity-induced states, we obtain that one of the scattering lengths indeed becomes much larger than the interatomic spacing for generic strong impurities (i. e., when impurity strength is of the order of the electronic bandwidth). This results in (i) a dramatic increase of the scattering cross-section and (ii) its strong energy dependence.

VIII. ACKNOWLEDGEMENTS

The author thanks A. C. Ferrari and S. Piscanec for stimulating discussions.

-
- * Electronic address: basko@sissa.it
- ¹ K. S. Novoselov, A. K. Geim, S. V. Morozov, D. Jiang, Y. Zhang, S. V. Dubonos, I. V. Grigorieva, and A. A. Firsov, *Science* **306**, 666 (2004).
 - ² J. C. Meyer, A. K. Geim, M. I. Katsnelson, K. S. Novoselov, T. J. Booth, and S. Roth, *Nature* **446**, 60 (2007).
 - ³ S. Gilje, S. Han, M. Wang, K. L. Wang, and R. B. Kaner, *Nano Lett.* **7**, 3394 (2007).
 - ⁴ C. Gómez-Navarro, R. T. Weitz, A. M. Bittner, M. Scolari, A. Mews, M. Burghard, and K. Kern, *Nano Lett.* **7**, 3499 (2007).
 - ⁵ T. C. Echtermeyer, M. C. Lemme, M. Baus, B. N. Szafranek, A. K. Geim, and H. Kurz, arXiv:0712.2026 (2008).
 - ⁶ Yu. G. Pogorelov, arXiv:cond-mat/0603327.
 - ⁷ Yu. V. Skrypnik and V. M. Loktev, *Phys. Rev. B* **73**, 241402(R) (2006).
 - ⁸ T. O. Wehling, A. V. Balatsky, M. I. Katsnelson, A. I. Lichtenstein, K. Scharnberg, and R. Wiesendanger, *Phys. Rev. B* **75**, 125425 (2007).
 - ⁹ C. Bena, *Phys. Rev. Lett.* **100**, 076601 (2008).
 - ¹⁰ I. L. Aleiner and K. B. Efetov, *Phys. Rev. Lett.* **97**, 236801 (2006).
 - ¹¹ J. O. Sofo, A. S. Chaudhari, and G. D. Barber, *Phys. Rev. B* **75**, 153401 (2007).
 - ¹² R. G. Newton, *Scattering Theory of Waves and Particles*, (McGraw Hill, 1966).
 - ¹³ D. P. DiVincenzo and E. J. Mele, *Phys. Rev. B* **29**, 1685 (1984).
 - ¹⁴ M. I. Katsnelson and K. S. Novoselov, *Solid State Commun.* **143**, 3 (2007).
 - ¹⁵ D. S. Novikov, *Phys. Rev. B* **76**, 245435 (2007).
 - ¹⁶ F. Guinea, arXiv:0805.3908 (2008).
 - ¹⁷ E. McCann, K. Kechedzhi, V. I. Falko, H. Suzuura, T. Ando, and B. L. Altshuler, *Phys. Rev. Lett.* **97**, 146805 (2006).
 - ¹⁸ M. Lax, *Symmetry Principles in Solid State and Molecular Physics* (Dover, New York, 2001 or Wiley, New York, 1974).
 - ¹⁹ For the states with negative energies, $s = -1$, the direction of the electron group velocity is opposite to that of momentum. Thus, for $s = -1$ the scattered part of the wave function (5) represents an *incoming* flux of electrons. However, we prefer to work with the T -matrix for the chronologically ordered Green's function $G(\mathbf{p}, \epsilon)$, defined in Eq. (9), rather than for the retarded Green's function $G^R(\mathbf{p}, \epsilon)$, the analytical continuation of $G(\mathbf{p}, \epsilon)$ from the positive semiaxis of ϵ through the upper complex half-plane of ϵ . For this purpose we work with the solutions (5) which correspond to outgoing waves for electrons if $s = 1$ and for holes if $s = -1$.
 - ²⁰ Expression (17) can be compared to analogous expressions for the case of scalar particles with parabolic spectrum determined by the mass m in the two- and three-dimensional cases [L. D. Landau and E. M. Lifshitz, *Quantum mechanics, non-relativistic theory*, (Pergamon Press, New York, 1977)]: $T_{3D}(\epsilon) = (2\pi l/m)/(1 + ipl)$, l being the scattering length, $p = \sqrt{2m\epsilon}$, and $T_{2D}(\epsilon) = (\pi/m)/[i\pi/2 - \ln(e^{\gamma} p r_0/2)]$.